JACS
JOURNAL OF THE AMERICAN CHEMICAL SOCIETY

COMMUNICATION

pubs.acs.org/JACS

Ultrathin Zirconium Disulfide Nanodiscs

Jung-tak Jang,[†] Sohee Jeong,[†] Jung-wook Seo,[†] Min-Cheol Kim,[†] Eunji Sim,[†] Yuhong Oh,[‡] Seunghoon Nam,[‡] Byungwoo Park,[‡] and Jinwoo Cheon*[,†]

[†]Department of Chemistry, Yonsei University, Seoul 120-749, Korea

[‡]Department of Materials Science and Engineering, and Research Institute of Advanced Materials, Seoul National University, Seoul 151-744, Korea

Supporting Information

ABSTRACT: We present a colloidal route for the synthesis of ultrathin ZrS_2 (UT-ZrS_2) nanodiscs that are ~1.6 nm thick and consist of approximately two unit cells of S−Zr−S. The lateral size of the discs can be tuned to 20, 35, or 60 nm while their thickness is kept constant. Under the appropriate conditions, these individual discs can self-assemble into face-to-face-stacked structures containing multiple discs. Because the S−Zr−S layers within individual discs are held together by weak van der Waals interactions, each UT-ZrS_2 disc provides spaces that can serve as host sites for intercalation. When we tested UT-ZrS_2 discs as anodic materials for Li^+ intercalation, they showed excellent nanoscale size effects, enhancing the discharge capacity by 230% and greatly improving the stability in comparison with bulk ZrS_2. The nanoscale size effect was especially prominent for their performance in fast charging/discharging cycles, where an 88% average recovery of reversible capacity was observed for UT-ZrS_2 discs with a lateral diameter of 20 nm. The nanoscale thickness and lateral size of UT-ZrS_2 discs are critical for fast and reliable intercalation cycling because those dimensions both increase the surface area and provide open edges that enhance the diffusion kinetics for guest molecules.

Ultrathin two-dimensional (2D) layered materials such as graphene and transition-metal chalcogenides (TMCs) hold special research interest because of the unique properties associated with their lateral anisotropy. Such materials hold the potential for a wide variety of characteristics, such as facile tuning of the electronic structure and the ability to intercalate a variety of molecules.[1,2]

In bulk forms, TMCs can exist in a diverse range of polytype structures (1T, 2H, 3R), and their intercalation capabilities are versatile.[1,3] For example, a typical TMC, titanium disulfide (TiS_2), has been reported to be an efficient lithium storage material,[4] drawing attention to the relationship between energy storage and intercalation compounds.[5] If these TMC layered materials can be scaled down to their most basic structural components of either a single layer or a few layers, it may be possible to observe new or pronounced nanoscale effects on their materials characteristics.

Although related nanostructures have been reported,[6] the synthesis of well-defined ultrathin TMC layered nanomaterials has been a challenging task. Their structures are anisotropic and have a high probability of containing dangling bonds at peripheral positions. The spheres or wires of TMCs synthesized by Tenne and co-workers[7] are beautiful structures, but those methods were not developed for the construction of ultrathin 2D disc or sheetlike structures. Hence, facile methods for the synthesis of ultrathin TMCs and the study of any new nanoscale properties associated with those size confinements remain topics of keen interest.

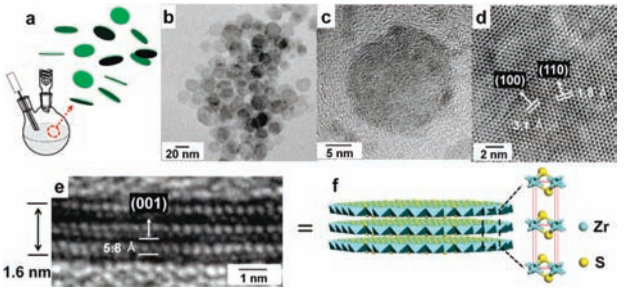

Figure 1. (a) Sketch of UT-ZrS_2 nanodiscs dispersed in solution. (b) Low- and (c) high-magnification TEM images of 20 nm single-crystalline UT-ZrS_2 nanodiscs lying flat on the TEM grid. (d) HRTEM image of a nanodisc showing (100) and (110) lattice fringes. (e) HRTEM side-view image of a nanodisc aligned with the electron beam, revealing a disc thickness of ~1.6 nm and 5.8 Å (001) lattice fringes. (f) Ball-and-stick model showing that a single disc corresponds to two unit cells with three S−Zr−S layers (Zr, sky-blue; S, yellow).

In this communication, we focus on the size-controlled synthesis of ultrathin ZrS_2 (UT-ZrS_2) as a case study among various potential ultrathin TMCs. UT-ZrS_2 nanodiscs were prepared by injecting carbon disulfide (CS_2) into a mixture of zirconium(IV) chloride ($ZrCl_4$) and oleylamine at 300 °C with stirring under argon atmosphere for 1 h. The H_2S generated by CS_2 and oleylamine reacted with $ZrCl_4$−oleylamine complexes to form UT-ZrS_2 nanodiscs dispersed in solution (Figure 1a).[8] The black colloidal products were isolated by centrifugation and washed with a mixture of *n*-butanol and hexane. Figure 1b shows a transmission electron microscopy (TEM) image of UT-ZrS_2 nanodiscs with an average diameter of 20 nm and a narrow size distribution ($\sigma \approx 12\%$). High-resolution TEM (HRTEM) analyses revealed the UT-ZrS_2 nanodiscs to be single-crystalline: a single UT-ZrS_2 nanodisc orthogonal to the direction of the electron beam gave lattice distances of 3.1 and 1.8 Å, corresponding to the (100) and (110) planes (Figure 1d). When oriented

Received: January 14, 2011
Published: May 03, 2011

dx.doi.org/10.1021/ja200400n | *J. Am. Chem. Soc.* 2011, 133, 7636–7639

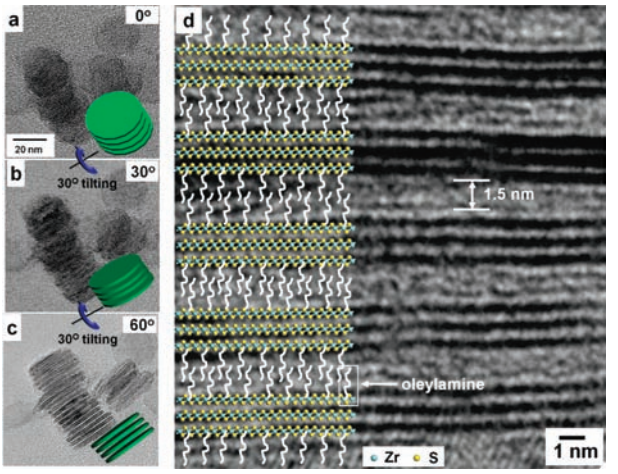

Figure 2. Self-assembled UT-ZrS_2 nanodiscs. (a−c) TEM images of assembled UT-ZrS_2 nanodiscs obtained by rotating the TEM holder from (a) 0 to (b) 30 and (c) 60°. (d) HRTEM side-view image of multiply stacked 1.6 nm thick UT-ZrS_2 nanodiscs showing a regularly spaced gap of ∼1.5 nm corresponding to the length of oleylamine surfactant layers.

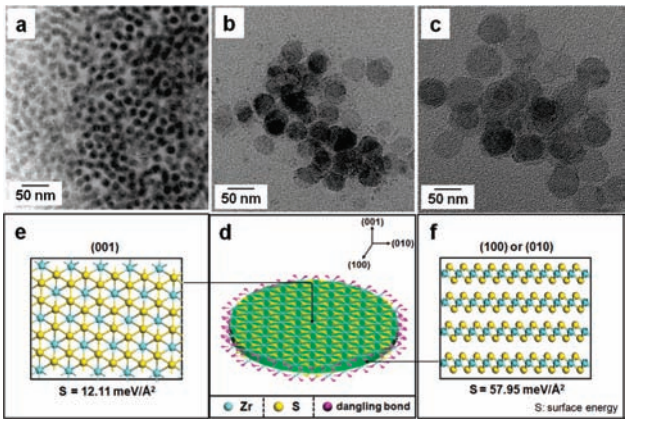

Figure 3. Size-controlled UT-ZrS_2 nanodiscs and calculated surface energies. (a−c) TEM images of UT-ZrS_2 nanodiscs with three different lateral sizes: (a) 20 nm ($\sigma \approx 12\%$); (b) 35 nm ($\sigma \approx 17\%$); (c) 60 nm ($\sigma \approx 21\%$). (d−f) Schematic diagrams of the UT-ZrS_2 nanodiscs shown as ball-and-stick models: (d) model of a nanodisc showing the dangling bonds at the peripheral positions (purple); (e) planar (001) facet and (f) lateral (100) or (010) facets of a nanodisc, which have calculated surface energies 12.11 and 57.95 meV/Å^2, respectively.

parallel to the direction of the electron beam (Figure 1e), each ZrS_2 disc was determined to be ∼1.6 nm thick with a 5.8 Å (001) lattice plane. This single UT-ZrS_2 disc comprised three layers of S−Zr−S repeating units, corresponding to two unit cells of 1T-type ZrS_2 (Figure 1e,f). X-ray diffraction patterns (Figure S1a in the Supporting Information) indicated that all of the peaks could be indexed to the hexagonal phase with *P*3*m*1 1T-type ZrS_2 and energy-dispersive X-ray spectroscopy (EDS) measurements confirmed the composition as 1:2 (Figure S1b).

These freestanding individual UT-ZrS_2 nanodiscs were dispersed in solution but easily underwent self-assembly upon a change from a nonpolar solvent such as toluene to a polar solvent such as chloroform. Assembled UT-ZrS_2 nanodiscs were examined by TEM tiling analyses (Figure 2a−c). Figure 2c shows the uniform stacking along the *c* axis, and the spacing between the discs was ∼1.5 nm (Figure 2d), which corresponds to the length of the oleylamine surfactant layers.[9] In polar solvents, UT-ZrS_2 nanodiscs aggregated into stacked structures to bury the nonpolar alkyl moieties of oleylamine.

At prolonged reaction times, the nanodiscs increased in lateral size. When the reaction time was increased from 1 to 3 h, the lateral size grew from 20 to 35 nm. After 6 h, we observed disc diameters of 60 nm (Figure 3a−c), but the thickness of the discs remained constant (∼1.6 nm). The discs obtained in these studies had relatively uniform lateral sizes. The surfactant and the surface energy appeared to play important roles in the formation of these ultrathin nanodisc structures. According to ab initio calculations that examined the structure optimization of ZrS_2 nanodiscs,[10] the surface energies (S) of the lateral facets such as (100) or (010) [$S_{(100)/(010)}$ = 57.95 meV/Å^2] and (110) [$S_{(110)}$ = 71.76 meV/Å^2] were 5−6 times larger than the surface energy of the planar (001) facet [$S_{(001)}$ = 12.11 meV/Å^2]. We largely attribute this difference to the dominance of unstable dangling bonds at the peripheral edges (Figure 3d, purple spheres). This large surface energy difference clearly explains the faster crystal growth rate in the lateral directions.[11] In addition, a previous report suggested that linear alkylamines tend to bind strongly to the hexagonal (001) surface, hindering the growth in the *c* direction.[12] Therefore, the combination of crystal surface anisotropy and the surfactant effect was critical in the formation of UT-ZrS_2 nanodiscs.

Because of the void space between their layers that allows UT-ZrS_2 nanodiscs to function as host materials, we tested their performance in Li^+ intercalation processes. First, UT-ZrS_2 nanodiscs were prepared and assembled into a coin-shaped electrode after heat treatment of the nanodiscs at 400 °C for 2 h under argon to remove the organic ligands. Subsequently, a half-cell electrochemical measurement was carried out (Figure 4a and Figure S2). The first reversible discharge capacity of 20 nm UT-ZrS_2 nanodiscs was 650 mA h g^{-1}, corresponding to intercalation of 3.8 mol of Li^+/mol of ZrS_2. The average discharge capacities of 20, 35, and 60 nm UT-ZrS_2 nanodiscs were 586, 527, and 433 mA h g^{-1}, respectively (Figure 4b,d). These values increased as the lateral size decreased, and the smallest nanodiscs (20 nm) showed a 230% enhancement in comparison with the value for bulk ZrS_2 materials (255 mA h g^{-1}).

We also examined the effects of charge and discharge rates in UT-ZrS_2 nanodiscs relative to bulk ZrS_2, when different current densities were applied sequentially (Figure 4c). The current density was increased up to 8-fold from 69 mA g^{-1} to 138, 276, and 552 mA g^{-1} and then decreased back to 69 m Ag^{-1} in the reverse sequence (Figure 4c). The retention capacity of the UT-ZrS_2 nanodiscs depended on size and was especially significant at higher current densities. For example, at the highest current density of 552 mA g^{-1} (dashed line box in Figure 4c), the capacity retention values were ∼80, ∼77, and ∼71% for nanodiscs with diameters of 20, 35, and 60 nm, respectively, while that of bulk ZrS_2 was ∼45%. After 50 cycles, the 20, 35, and 60 nm nanodiscs showed stabilized capacity retention values of 86, 84, and 80%, respectively (Figure 4c), while the capacity of bulk ZrS_2 declined continuously over time and reached a final value of 39%. The UT-ZrS_2 nanodiscs may acquire these advantageous properties partly because of their large surface areas (171.6, 131, and 78 m^2 g^{-1} for 20, 35, and 60 nm nanodiscs) relative to bulk ZrS_2 (8.1 m^2 g^{-1}) (Figure S3).

dx.doi.org/10.1021/ja200400n |*J. Am. Chem. Soc.* 2011, 133, 7636–7639

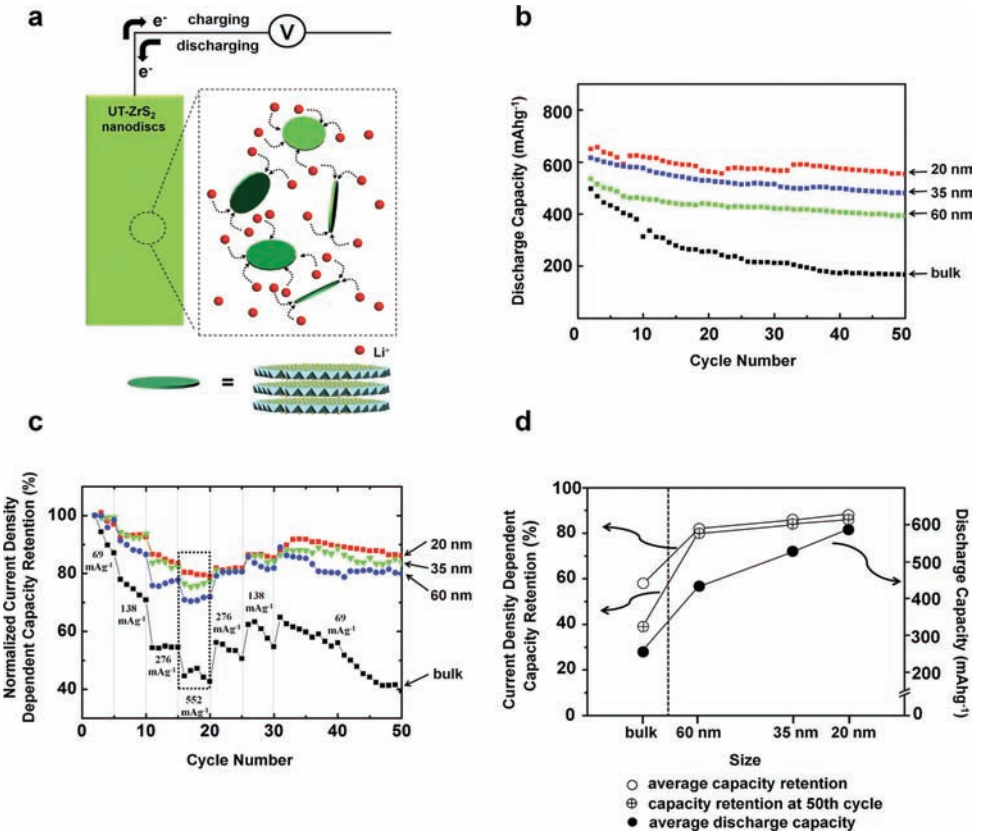

Figure 4. Size-dependent electrochemical properties of UT-ZrS_2 nanodiscs in Li^+ intercalation studies. (a) Schematic diagram of UT-ZrS_2 nanodiscs as anodic materials. (b) Discharge capacity profiles of the UT-ZrS_2 nanodiscs and bulk ZrS_2. (c) Current-density-dependent capacity profiles of the UT-ZrS_2 nanodiscs and bulk ZrS_2 at current densities of 69, 138, 276, and 552 mAg^{-1}. (d) Summary graphs of Li^+ charge/discharge capacity changes as functions of nanodisc size.

Among the three sizes of UT-ZrS_2 discs, the smallest (20 nm) showed the best capacity retention after the multiple sequences of fast and slow charging/discharging cycles (Figure 4d). On the basis of our observations and those of other groups, the rapid capacity fade reported for bulk materials is especially common at high current densities.[13] The size-dependent effects observed for these UT-ZrS_2 nanodiscs clearly demonstrate their merits for high-performance applications. The increased surface area and openness within these nanostructures facilitate Li^+ insertion and removal and enhance the Li^+ diffusion kinetics.

In summary, we have demonstrated the synthesis of ultrathin ZrS_2 nanodiscs whose lateral size can be easily modulated. Such ultrathin nanodiscs are highly functional as host materials where nanoscale size effects are significant, and we tested them as anode materials for intercalation processes. Such materials are not limited to the host−guest chemistry shown in this study; these ultrathin 2D materials can be useful in a variety of scientific areas, including catalysis and solid-state lubrication. In addition, this synthetic process is simple and could be easily extended to the preparation of other types of ultrathin metal chalcogenides.

■ ASSOCIATED CONTENT

Supporting Information. Synthetic methods, structural characterizations, surface energy calculations, discharge voltage profiles, surface area measurements, and annealing experiments on ZrS_2. This material is available free of charge via the Internet at http://pubs.acs.org.

■ AUTHOR INFORMATION

Corresponding Author
jcheon@yonsei.ac.kr

■ ACKNOWLEDGMENT

We thank W. Cho and Prof. M. Oh for the surface area measurement and J.-G. Kim for TEM analyses [KBSI-HVEM (JEM-ARM1300S)]. This work was supported in part by the Creative Research Initiative (2010-0018286), the WCU Program (R32-2009-10217), and the BK21 Project (to J.C.); the NRF (2010-0017172) (to E.S.); and the NRF (2010-0029065) and the WCU Program (R31-2008-000-10075-0) (to B.P.)

■ REFERENCES

(1) (a) Dresselhaus, M. S. *Intercalation in Layered Materials*; NATO ASI Series; Plenum Press: New York, 1986. (b) Mattheiss, L. F. *Phys. Rev. B* **1973**, *8*, 3719–3740.(c) Singleton, J. *Band Theory and Electronic Properties of Solids*; Oxford University Press: Oxford, U.K., 2001.

(2) (a) Geim, A. K.; Novoselov, K. S. *Nature* **2007**, *6*, 183–191. (b) Choucair, M.; Thordarson, P.; Stride, J. A. *Nat. Nanotechnol.* **2008**, *4*, 30–33. (c) Schedin, F.; Geim, A. K.; Morozov, S. V.; Hill, E. W.; Blake, P.; Katsnelson, M. I.; Novoselov, K. S. *Nat. Mater.* **2007**, *6*, 652–655.

(3) (a) Wilson, J. A.; Yoffe, A. D. *Adv. Phys.* **1969**, *18*, 193–335. (b) Friend, R. H.; Yoffe, A. D. *Adv. Phys.* **1987**, *36*, 1–94.

(4) Whittingham, M. S. *Science* **1976**, *192*, 1126–1127.

(5) (a) Arico, A. S.; Bruce, P.; Scrosati, B.; Trrascon, J.; Schalkwijk, W. V. *Nature* **2005**, *4*, 366–377. (b) Winter, M.; Besenhard, J. O.; Spahr,

M. E.; Novak, P. *Adv. Mater.* **1998**, *10*, 725–763. (c) Chen, J.; Cheng, F. *Acc. Chem. Res.* **2009**, *42*, 713–723.(d) Linden, D.; Reddy, T. B. *Handbook of Batteries*, 3rd ed.; McGraw-Hill: New York, 2002. (e) Chhowalla, M.; Amaratunga, G. A. J. *Nature* **2000**, *407*, 164–167.

(6) (a) Huo, Z.; Tsung, C.; Huang, W.; Fardy, M.; Yan, R.; Zhang, X.; Li, Y.; Yang, P. *Nano Lett.* **2009**, *9*, 1260–1264. (b) Park, K. H.; Choi, J.; Kim, H. J.; Oh, D.-H.; Ahn, J. R.; Son, S. U. *Small* **2008**, *4*, 945–950. (c) Sigman, M. B.; Ghezelbash, A.; Hanrath, T.; Saunders, A. E.; Lee, F.; Korgel, B. A. *J. Am. Chem. Soc.* **2003**, *125*, 16050–16057. (d) Saunder, A. E.; Ghezelbash, A.; Smilgies, D.-M.; Sigman, M. B.; Korgel, B. A. *Nano Lett.* **2006**, *6*, 2959–2963.

(7) (a) Tenne, R. *Chem.—Eur. J.* **2002**, *8*, 5297–5304. (b) Zak, A.; Feldman, Y.; Alperovich, V.; Rosentsveig, R.; Tenne, R. *J. Am. Chem. Soc.* **2000**, *122*, 11108–11116. (c) Tenne, R.; Homoyonfer, M.; Feldman, Y. *Chem. Mater.* **1998**, *10*, 3225–3238. (d) Feldman, Y.; Wasserman, E.; Srolovitz, J.; Tenne, R. *Science* **1995**, *267*, 222–225.

(8) Ballabeni, M.; Ballini, R.; Bigi, F.; Maggi, R.; Parrini, M.; Predieri, G.; Sartori, G. *J. Org. Chem.* **1999**, *64*, 1029–1032.

(9) (a) Du, W.; Qian, X.; Ma, X.; Gong, Q.; Cao, H.; Yin, J. *Chem.—Eur. J.* **2007**, *13*, 3241–3247. (b) Bain, C. D.; Evall, J.; Whitesides, G. M. *J. Am. Chem. Soc.* **1989**, *111*, 7155–7164.

(10) (a) Zhang, S. B.; Wei, S.-H. *Phys. Rev. Lett.* **2004**, *92*, No. 086102. (b) Manna, L.; Wang, L. W.; Cingolani, R.; Alivisatos, A. P. *J. Phys. Chem. B* **2005**, *109*, 6183–6192. (c) Soler, J. M.; Artacho, E.; Gale, J. D.; García, A.; Junquera, J.; Ordejón, P.; Portal, S. *J. Phys.: Condens. Matter* **2002**, *14*, 2745–2779.

(11) *Annual Review of Nano Research*, Vol. 2; Cao, G., Brinker, C. J., Eds.; World Scientific Publishing: Singapore, 2008.

(12) (a) Osiecki, R. J. H. M.; Pisharody, C. R.; DiSalvo, F. J.; Geballe, T. H. *Science* **1971**, *174*, 493–497. (b) Ha, B.; Char, K.; Jeon, H. S. *J. Phys. Chem. B* **2005**, *109*, 24434–24440.

(13) (a) Yamada, A.; Kim, S. C.; Hinokuma, K. *J. Electochem. Soc.* **2001**, *148*, A224–A229. (b) Ning, G.; Haran, B.; Popov, B. N. *J. Power Sources* **2003**, *117*, 160–169. (c) Lee, Y.; Kim, M. G.; Cho, J. *Nano Lett.* **2008**, *8*, 957–961.